Correction

Correction for "Fresnel drag in space–time-modulated metamaterials," by Paloma A. Huidobro, Emanuele Galiffi, Sébastien Guenneau, Richard V. Craster, and J. B. Pendry, which was first published November 25, 2019; 10.1073/pnas.1915027116 (*Proc. Natl. Acad. Sci. U.S.A.* **116**, 24943–24948).

The authors wish to note the following: "The Lorentz transformation of the magneto-electric coupling, Eq. **24**, should be

$$\xi = v \frac{\epsilon' \mu' - 1/c_0^2}{1 - \epsilon' \mu' v^2}$$

"In addition, in the expressions for the transformation of the permittivity and permeability, Eqs. **21** and **22**, c_m should be replaced by c_0. Note that in our units $c_0 = 1$, and v is also assumed to be normalized by the speed of light.

"With that set of equations (**21**, **22**, and the amended version of **24**), the parameters of the equivalent moving medium (ϵ', μ' and v_D) can be rederived. To second order in the modulation strength, α, the resulting expressions yield the same as Eqs. **25** and **26** in the main text, with the exception of a prefactor in the drag velocity,

$$v_D \approx -\alpha^2 \frac{1}{c_0^{-2} - c_m^{-2}} \left(\frac{2g\Omega}{c_m^2 g^2 - \Omega^2} \right).$$

"The above equation for the drag velocity is naturally ill-defined for $c_m = 1$, as this implies the modulation of a vacuum. The above changes do not change any of the conclusions in the paper."

Fresnel drag in space–time-modulated metamaterials

Paloma A. Huidobro[a,1], Emanuele Galiffi[b], Sébastien Guenneau[c,d], Richard V. Craster[c], and J. B. Pendry[b,1]

[a]Instituto de Telecomunicações, Insituto Superior Técnico, University of Lisbon, 1049-001 Lisbon, Portugal; [b]Condensed Matter Theory Group, The Blackett Laboratory, Imperial College, SW7 2AZ, London, United Kingdom; [c]Department of Mathematics, Imperial College London, London SW7 2AZ, United Kingdom; and [d]Institut Fresnel, Aix-Marseille University, CNRS, Centrale Marseille, 13013 Marseille, France

A moving medium drags light along with it as measured by Fizeau and explained by Einstein's theory of special relativity. Here we show that the same effect can be obtained in a situation where there is no physical motion of the medium. Modulations of both the permittivity and permeability, phased in space and time in the form of traveling waves, are the basis of our model. Space–time metamaterials are represented by effective bianisotropic parameters, which can in turn be mapped to a moving homogeneous medium. Hence these metamaterials mimic a relativistic effect without the need for any actual material motion. We discuss how both the permittivity and permeability need to be modulated to achieve these effects, and we present an equivalent transmission line model.

metamaterials | space–time modulations | Fresnel drag | nonreciprocity

In 1818 Fresnel produced the aether drag hypothesis: A moving fluid appears to "drag" light along so that light traveling in opposite directions to the fluid flow would have different velocities (1). His extra velocity was related to but not equal to the velocity of the fluid. Although Fresnel's derivation was flawed, Fizeau in 1851 measured the drag effect and confirmed Fresnel's formula (2). A correct explanation followed in the wake of Einstein's theory of relativity, of which the aether drag experiment is one of the cornerstones (3).

While it may seem that physical movement of the fluid is an essential part of aether drag (4, 5), here we come to the surprising conclusion that a time-dependent system involving no physical movement of a medium can also produce a drag effect. We calculate the shifted dispersion surface and show that the system can be represented as a bianisotropic metamaterial (Fig. 1), whose magnetoelectric coupling vanishes when either the dielectric or the magnetic modulation is switched off. Finally we propose a simple experiment which would demonstrate our results.

We consider a metamaterial whose permittivity and permeability are modulated in space and time following a traveling-wave form,

$$\epsilon(x, t) = \epsilon_m [1 + 2\alpha_e \cos(gx - \Omega t)], \quad [1]$$

$$\mu(x, t) = \mu_m [1 + 2\alpha_m \cos(gx - \Omega t)], \quad [2]$$

where g and Ω are the spatial and temporal frequencies, $\alpha_{e,m}$ are the electric and magnetic modulation strengths, and ϵ_m and μ_m are the background relative permittivity and permeability of the medium. The profile moves with a phase velocity of $c_g = \Omega/g$ but we emphasize that the medium itself does not move: As a consequence the phase velocity can take any value between zero and infinity without violating special relativity. We concern ourselves with low-frequency, long-wavelength excitations, enabling the medium to be represented as a metamaterial with effective medium parameters which we calculate. Importantly, the drift velocity appearing in space–time metamaterials differs from both the modulation phase velocity and the conventional Fresnel–Einstein result, and it can even oppose the modulation phase velocity, when this is lower than the speed of light c_m in the unmodulated medium.

Modulation of the electric permittivity in space and time has attracted much attention, as it gives rise to a plethora of exotic

effects ranging from frequency-momentum transitions (6–8) to compression and amplification of electromagnetic signals (9–15), one-way hyperbolic metasurfaces (16), and even non-Hermitian and topological phenomena (17–21). The directionality of space–time modulations such as traveling-wave modulations breaks time-reversal symmetry, which is reflected in nonreciprocal band diagrams (4). The breaking of reciprocity has been exploited in the realization of photonic isolators and circulators without the need of external static magnetic biasing (22–24). Recently, it was shown that in-phase modulations of the permittivity and the permeability with the same strength result in the closing of the high-frequency band gaps, at the same time as keeping the nonreciprocal character of these systems (25). Here we further show that this nonreciprocity is in fact accompanied by a Fresnel drag and we present an effective medium model that illuminates its origin.

Results and Discussion

Effective Medium Theory of Space–Time Metamaterials. Maxwell's equations in space–time-modulated media,

$$\nabla \times \mathbf{E} = -\frac{\partial \mathbf{B}}{\partial t} = -\frac{\partial}{\partial t} [\mu(x, t)\mu_0 \mathbf{H}], \quad [3]$$

$$\nabla \times \mathbf{H} = \frac{\partial \mathbf{D}}{\partial t} = \frac{\partial}{\partial t} [\epsilon(x, t)\epsilon_0 \mathbf{E}], \quad [4]$$

with ϵ_0 and μ_0 determining the speed of light in vacuum as $c_0 = 1/\sqrt{\epsilon_0\mu_0}$, can be solved by taking a Bloch–Floquet ansatz (9),

$$\mathbf{E} = \sum_n \mathbf{E}_n e^{i(k+ng)x + ik_y y - i(\omega + n\Omega)t}, \quad [5]$$

$$\mathbf{H} = \sum_n \mathbf{H}_n e^{i(k+ng)x + ik_y y - i(\omega + n\Omega)t}, \quad [6]$$

Significance

Space–time-dependent electromagnetic media, whose constitutive parameters are directionally biased in space and time, are a topic of current enormous interest across physics. Here we address a problem of fundamental relevance: the similarities and differences between such modulated materials and the classic problem of moving media. We establish that, surprisingly, the Fresnel drag effect of light in moving media, dictated by special relativity, is also present in modulated media, fully resolving this paradox with an analytical approach. We discuss how nonreciprocity can emerge at vanishing frequency. While we focus on electromagnetism, our findings can be extended to other wave systems.
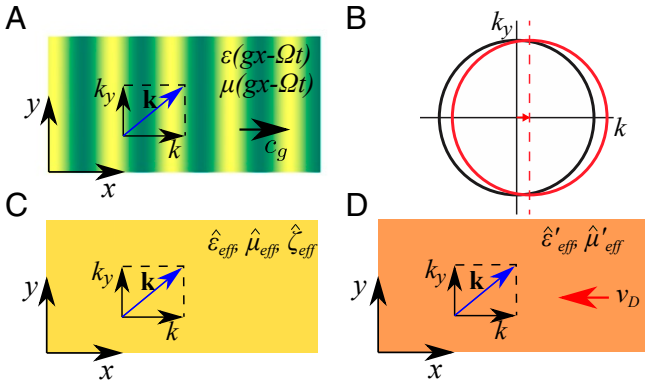
Fig. 1. Fresnel drag in space–time-modulated metamaterials. (*A*) A wave propagates in a medium with space–time traveling-wave–modulated permittivity and permeability. The wave vectors k and k_y are along the direction of the space–time grating and orthogonal to it, respectively. (*B*) Sketch of the low-frequency dispersion surface in the (k, k_y) plane. The isofrequency contours are ellipses centered at a finite value of k, reflecting a Fresnel drag effect along the modulation direction. (*C*) In the long-wavelength limit the space–time-modulated medium is mapped into a magnetoelectric medium with anisotropic effective permittivity $\hat{\varepsilon}_{\text{eff}}$, permeability $\hat{\mu}_{\text{eff}}$, and magnetoelectric coupling $\hat{\zeta}_{\text{eff}}$ parameters. (*D*) Equivalent moving medium interpretation: uniaxial medium with anisotropic effective permittivity $\hat{\varepsilon}'_{\text{eff}}$ and permeability $\hat{\mu}'_{\text{eff}}$ moving with velocity v_D. Notice that the direction of the drift velocity in *D* corresponds to the case of subluminal modulations ($c_m g < \Omega$), and it flips sign in the superluminal regime ($c_m g > \Omega$).

with ω the wave frequency and k and k_y the wave vectors as defined in Fig. 1. Assuming an s-polarized wave without loss of generality, this procedure leads to a system of equations for the E_z and H_y components of the electromagnetic fields. An eigenvalue equation can be written as

$$k \begin{bmatrix} \mathbf{E} \\ \mathbf{H} \end{bmatrix} = \begin{bmatrix} \mathbf{M}^{EE} & \mathbf{M}^{EH} \\ \mathbf{M}^{HE} & \mathbf{M}^{HH} \end{bmatrix} \begin{bmatrix} \mathbf{E} \\ \mathbf{H} \end{bmatrix}, \qquad [7]$$

where **E** and **H** now stand for column vectors of the Bloch–Floquet amplitudes of E_z and H_y, respectively. The block matri-

ces in Eq. **7** depend on ω and satisfy $\mathbf{M}^{EE} = \mathbf{M}^{HH}$ and their expressions are given in *Materials and Methods*.

It is useful to rewrite the eigenvalue equations on the basis of forward and backward propagating waves as follows:

$$k \begin{bmatrix} \mathbf{E} + \mathbf{H} \\ \mathbf{E} - \mathbf{H} \end{bmatrix} = \begin{bmatrix} \mathbf{M}^{++} & \mathbf{M}^{+-} \\ -\mathbf{M}^{+-} & \mathbf{M}^{--} \end{bmatrix} \begin{bmatrix} \mathbf{E} + \mathbf{H} \\ \mathbf{E} - \mathbf{H} \end{bmatrix}. \qquad [8]$$

Here, $\mathbf{M}^{++}_{--} = \mathbf{M}^{EE} \pm \frac{1}{2} \left(\mathbf{M}^{EH} + \mathbf{M}^{HE} \right)$ and $\mathbf{M}^{+-} = -\frac{1}{2} \left(\mathbf{M}^{EH} - \mathbf{M}^{HE} \right)$. Solving Eq. **8** yields the dispersion relation of the system, $k(\omega)$.

In the long-wavelength limit, the dispersion relation can be written analytically by considering only 3 neighboring modes in the eigenvalue equation and approximating $\omega \ll \Omega$, $k \ll g$. This gives

$$\beta^2 \omega^2 = \kappa^2 k_y^2 + (k - \delta \omega)^2, \qquad [9]$$

where

$$\beta^2 = c_m^{-2} \left(1 + \alpha_e^2 \frac{2\Omega^2}{c_m^2 g^2 - \Omega^2} \right) \left(1 + \alpha_m^2 \frac{2\Omega^2}{c_m^2 g^2 - \Omega^2} \right), \qquad [10]$$

$$\kappa^2 = 1 + \alpha_m^2 \frac{2\Omega^2}{c_m^2 g^2 - \Omega^2}, \qquad [11]$$

$$\delta = \alpha_e \alpha_m \frac{2g\Omega}{c_m^2 g^2 - \Omega^2}, \qquad [12]$$

and $c_m^2 = 1/\epsilon_m \mu_m$. Hence the dispersion surfaces are approximately circles of radius $\omega\beta$ and whose center is displaced from the origin along the k axis by $\delta\omega$. This produces an asymmetry with respect to the $k = 0$ axis, since the dispersion surfaces are displaced along the direction of the modulation, as shown in Fig. 2 and discussed below in detail.

Fresnel Drag. Here we interpret the displacement of the dispersion surface shown above as an aether drag, which is well known to affect light propagating through moving media (26). In the conventional Fresnel drag effect, moving matter drags light, imparting an extra speed to it. Measured by Fizeau in 1851, Einstein noticed that it is a relativistic effect and that the
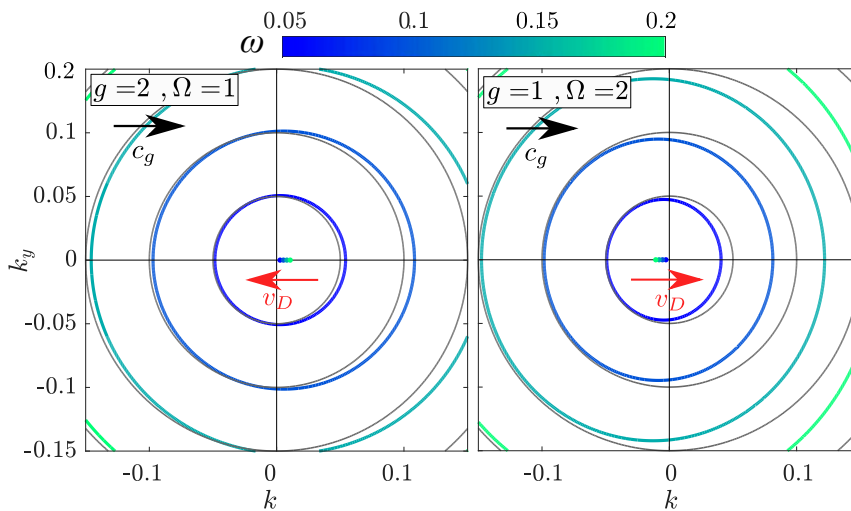

Fig. 2. Fresnel drag in space–time ϵ- and μ-modulated metamaterials with $\alpha_e = \alpha_m = 0.2$. The isofrequency contours in the (k, k_y) plane are shown for (*Left*) subluminal ($c_m g > \Omega$) and (*Right*) superluminal ($\Omega > c_m g$) modulations, with $c_m = 1$. Note the change in radius compared to the dispersion in unmodulated media (gray circles) and the displacement along the k axis. In the subluminal case, the space–time modulation drags the waves in the direction opposite to its phase velocity (the effective drift velocity, v_D, sketched in red, is antiparallel to the modulation phase velocity, c_g, sketched in black), while the drift velocity flips sign (v_D parallel to c_g) upon a superluminal modulation $c_g > c_m$. Note the displacement of the centers of the contours, which are plotted with dots of the same color as the corresponding contour. The group velocity direction is given by the normal to these dispersion surfaces.

Huidobro et al.

speed of light in the medium can be calculated from Lorentz's velocity formula. While it may seem that moving matter is needed to produce a Fresnel drag, our results show that it can also emerge in the presence of space–time modulations, where the modulation profile appears to be moving at a certain speed despite the absence of moving matter. This surprising result can be understood from our effective medium theory. In fact, as we show below, the space–time-modulated metamaterial can be equivalently represented by a moving medium, which explains the light-dragging effect. Interestingly, the effective drift is present as long as $\delta \neq 0$; i.e., $\alpha_e \cdot \alpha_m \neq 0$ and $g \cdot \Omega \neq 0$. In other words, the Fresnel drag in space–time metamaterials emerges when both the permittivity and permeability are modulated and when the modulations have nonzero spatial and temporal frequencies.

The isofrequency contours given by Eq. 9 are shown in Fig. 2 for 2 examples of space–time metamaterials: with subluminal (Fig. 2, *Left*) and superluminal (Fig. 2, *Right*) modulation speeds. The modulation strength is chosen in both cases as $\alpha_e = \alpha_m = 0.2$ such that the permittivity and permeability are equally modulated. For comparison, we also show the isofrequency contours of unmodulated media ($\omega^2/c_m^2 = k^2 + k_y^2$; Fig. 2, gray lines). Here and in all of the results shown in the paper we take $\epsilon_m = \mu_m = 1$, so that $c_m = 1$. It can be seen how in the presence of the modulation, the circular contours change shape, and their center, which is plotted as a dot of the same color as the corresponding contour, gets displaced along the k axis. This shows the Fresnel drag in space–time metamaterials. Interestingly, when the modulation speed is subluminal, the isofrequency contours are displaced in the direction of the modulation's phase velocity (Fig. 2, *Left*). On the other hand, when the modulation is superluminal, the contours are displaced in the direction opposite to the modulation's phase velocity (Fig. 2, *Right*). In other words, given a space–time variation of ϵ and μ, the direction of the Fresnel drag can be switched by changing between subluminal and superluminal modulations. Remarkably, this implies that the direction of the Fresnel drag velocity is antiparallel to the phase velocity of the modulation in the subluminal case and parallel to it in the superluminal case. This seemingly counterintuitive fact is fully justified below.

In addition, the extent of the Fresnel effect in these media depends on the magnitude of the modulation speed. It increases as c_g increases from $c_g = 0$ in the subluminal regime and as c_g decreases from ∞ in the superluminal regime. As the luminal modulation regime $c_g \rightarrow c_m$ is approached, however, strong interaction between multiple bands results in an unstable regime dominated by intraband photonic transitions (9, 15), which spoils the separation of length scales needed for long-wavelength homogenization.

Effective Bianisotropic Parameters and Nonreciprocity. Next we derive the effective medium parameters of the space–time metamaterial. We start by noting that the dispersion relation of waves in the space–time-modulated medium, Eq. 9, is of the form of the dispersion of waves in a bianisotropic medium with uniaxial ϵ and μ,

$$\boldsymbol{\epsilon} = \begin{bmatrix} \epsilon_x & 0 & 0 \\ 0 & \epsilon & 0 \\ 0 & 0 & \epsilon \end{bmatrix}; \ \boldsymbol{\mu} = \begin{bmatrix} \mu_x & 0 & 0 \\ 0 & \mu & 0 \\ 0 & 0 & \mu \end{bmatrix}, \quad [\mathbf{13}]$$

and magnetoelectric coupling,

$$\boldsymbol{\xi} = \boldsymbol{\zeta}^T = \begin{bmatrix} 0 & 0 & 0 \\ 0 & 0 & +\xi \\ 0 & -\xi & 0 \end{bmatrix}. \quad [\mathbf{14}]$$

For s-polarized waves we have in this case

$$\mu \mu_0 \epsilon \epsilon_0 \omega^2 = \frac{\mu}{\mu_x} k_y^2 + (k - \xi \omega)^2. \quad [\mathbf{15}]$$

By comparing to Eq. 9 we can identify a set of effective medium parameters for the space–time-modulated metamaterial,

$$\epsilon_x = \mu_x = 1, \quad [\mathbf{16}]$$

$$\epsilon = 1 + \alpha_e^2 \frac{2\Omega^2}{c_m^2 g^2 - \Omega^2}, \quad [\mathbf{17}]$$

$$\mu = 1 + \alpha_m^2 \frac{2\Omega^2}{c_m^2 g^2 - \Omega^2}, \quad [\mathbf{18}]$$

$$\xi = \alpha_e \alpha_m \frac{2g\Omega}{c_m^2 g^2 - \Omega^2}. \quad [\mathbf{19}]$$

This shows that the modulated medium can be represented by an effective bianisotropic material. Interestingly, the magnetoelectric coupling vanishes if the modulation is only spatial ($\Omega = 0$) or only temporal ($g = 0$) or if only one of the electromagnetic parameters is modulated; i.e., $\alpha_e \cdot \alpha_m = 0$. We also note in passing that space–time metamaterials with only ϵ or μ modulations are mapped to uniaxial media (without any magnetoelectric coupling).

The magnitude of ξ is presented in Fig. 3, as a function of the electric and magnetic modulation strengths. When changing from a subluminal (Fig. 3, *Left*) to a superluminal (Fig. 3, *Right*) modulation speed, the magnetoelectric coupling changes sign, in agreement with the reverse directions obtained for the Fresnel drag. In addition, we can conclude from this plot that a phase difference of π between the ϵ and μ modulations also reverses the direction of the aether drag with respect to in-phase modulations, since ξ changes sign with $sign(\alpha_e \cdot \alpha_m)$.

In agreement with the effective bianisotropic parameters, the dispersion surfaces shown in Fig. 2 represent nonreciprocal dispersion relations, a result of the time-reversal symmetry breaking induced by the modulation. From Eq. 9 we can explicitly write dispersion relations for forward and backward propagating waves,

$$k_\pm = \delta\omega \pm \sqrt{\beta^2 \omega^2 - \kappa^2 k_y^2}. \quad [\mathbf{20}]$$

Clearly, when $\delta \neq 0$ ($\xi \neq 0$), the 2 branches are asymmetric with respect to $k = 0$; that is, the system is nonreciprocal when both
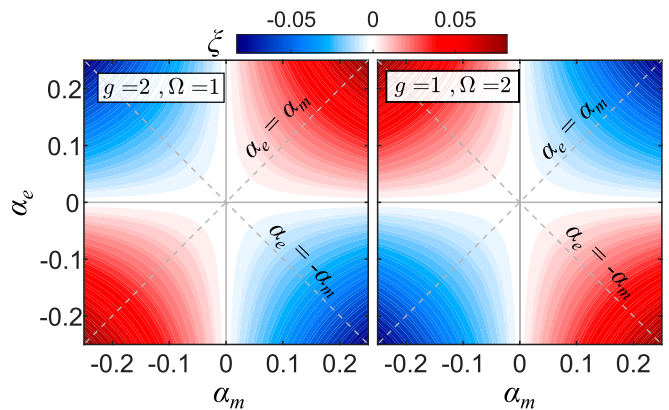

Fig. 3. Nonreciprocity map in the α_e, α_m parameter space for subluminal (*Left*) and superluminal (*Right*) gratings, with $c_m = 1$. The color map shows effective magnetoelectric coupling, ξ, which is equal to δ and which also gives the difference in the inverse of phase velocities between forward and backward propagating waves, $\Delta = (k_+ - |k_-|)/\omega = 2\delta$. It is seen that it is necessary to modulate both parameters to achieve nonreciprocity in the long-wavelength limit.

α_e and α_m are nonzero. For waves traveling in the direction of the modulation, $k_y = 0$, it is easy to see that the difference between the wave vectors of forward and backward waves divided by frequency is given by $\Delta = 2\delta = 2\xi$. Hence, we can interpret Fig. 3 as a map of the strength of nonreciprocity. From this we confirm that a nonreciprocal response requires both permittivity and permeability modulations and that for a fixed total modulation strength, $\alpha_e^2 + \alpha_m^2 = \alpha^2$, nonreciprocity is maximized by $\alpha_e = \alpha_m$.

Equivalent Moving Medium. The link between moving media and bianisotropic effective parameters has been shown in the past (27, 28). Hence, since the space–time-modulated medium can be represented by effective bianisotropic parameters, it can also be linked to an equivalent moving medium. Below we derive the speed of the equivalent moving medium.

Consider a moving uniaxial medium with parameters $\hat{\epsilon}' = \text{diag}(\epsilon'_x, \epsilon', \epsilon')$, $\hat{\mu}' = \text{diag}(\mu'_x, \mu', \mu')$, moving along the x axis with speed v. Lorentz transformations tell us that in the moving frame the permittivity and permeability change as (26)

$$\epsilon_x = \epsilon'_x, \quad \epsilon = \epsilon' \frac{1 - v^2/c_m^2}{1 - \epsilon'\mu'v^2/c_m^2}, \qquad [21]$$

$$\mu_x = \mu'_x, \quad \mu = \mu' \frac{1 - v^2/c_m^2}{1 - \epsilon'\mu'v^2/c_m^2}. \qquad [22]$$

Also, the electric and magnetic fields in the moving frame are coupled through magnetoelectric tensors,

$$\boldsymbol{\xi} = \boldsymbol{\zeta}^T = \begin{bmatrix} 0 & 0 & 0 \\ 0 & 0 & +\xi \\ 0 & -\xi & 0 \end{bmatrix}, \qquad [23]$$

where

$$\xi = \frac{v}{c_m} \frac{\epsilon'\mu' - 1}{\epsilon'\mu' - v^2/c_m^2}. \qquad [24]$$

By mapping the tensors (21–23) to the set of effective bianisotropic parameters in Eqs. **16–19**, we determine

$$v_D \approx -\xi c_m^2 \epsilon' \mu' \approx -\alpha^2 \frac{2c_m^2 g\Omega}{c_m^2 g^2 - \Omega^2}, \qquad [25]$$

and

$$\epsilon' = \mu' \approx \frac{\epsilon}{1 - v^2/c_m^2} \approx 1 + \alpha^2 \frac{2\Omega^2}{c_m^2 g^2 - \Omega^2}, \qquad [26]$$

where we have restricted ourselves to the case where $\epsilon = \mu$, i.e., $\alpha_e = \alpha_m = \alpha$, for simplicity. The velocity v_D is the drag velocity that light experiences in the space–time metamaterial. This justifies our interpretation of the isofrequency contours in Fig. 2 as an aether drag.

It is clear from Eq. **25** that when the modulation is subluminal ($c_m g > \Omega$), $v_D < 0$, such that the effective medium moves in the opposite direction to the phase velocity of the modulation. Hence, forward propagating modes slow down in the presence of subluminal space–time modulations, and backward propagating modes speed up. On the other hand, for superluminal modulations ($c_m g < \Omega$), $v_D > 0$, such that the drag velocity points in the same direction as the modulation's phase velocity. In this case, forward waves speed up and backward waves slow down. We remark here that there are 2 effects at work in the space–time-modulated metamaterial. In addition to the Fresnel drag, there is an increase/reduction in the effective permittivity and permeability for subluminal/superluminal media, as can be seen in Eq. **26**. Hence, the slowing down or speeding up of the waves is in relation to waves propagating in the
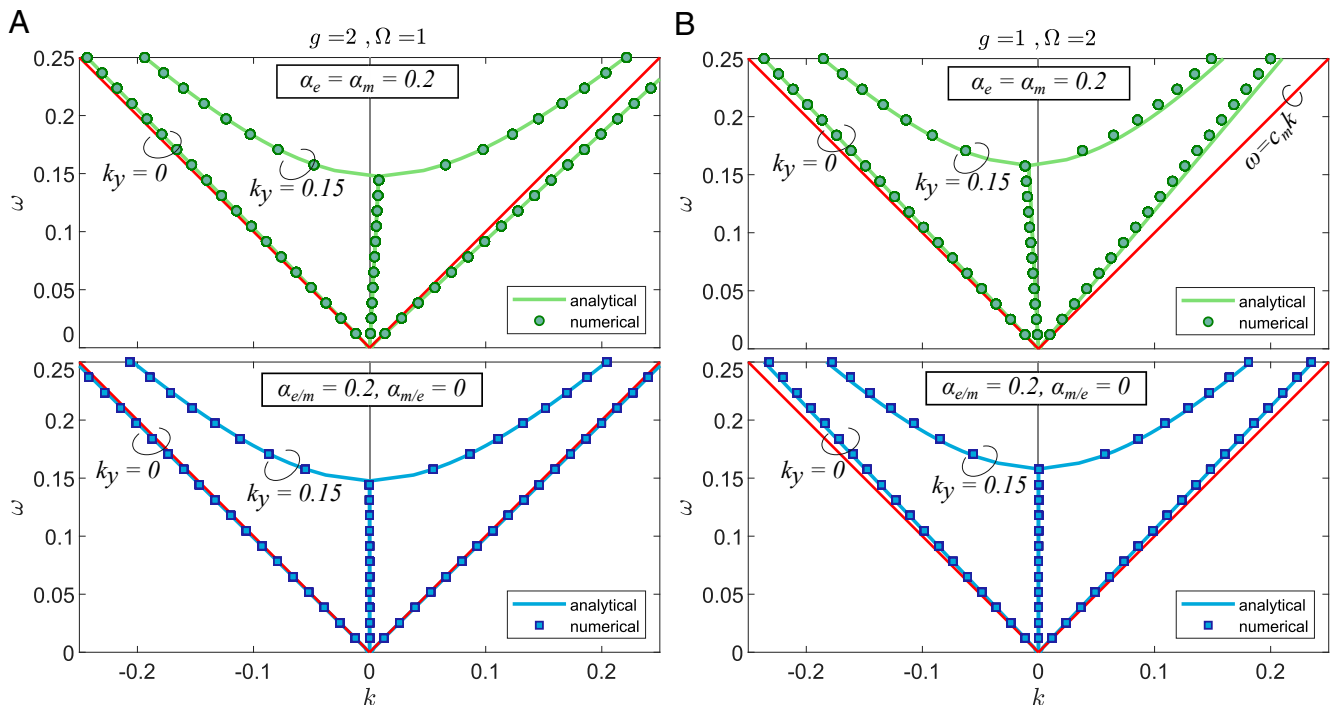

Fig. 4. Dispersion relations for $k_y = 0$ and $k_y = 0.15$, for subluminal (*A*) and superluminal (*B*) metamaterials, with $c_m = 1$. *A* and *B*, *Top* show how ϵ and μ traveling-wave modulations yield nonreciprocal dispersion. The permittivity and permeability modulations are set equal, $\alpha_e = \alpha_m = 0.2$. *A* and *B*, *Bottom* show how when only one of the parameters is modulated with the same strength as before ($\alpha_e = 0.2$ or $\alpha_m = 0.2$) and the other one is kept constant ($\alpha_m = 0$ or $\alpha_e = 0$), the system is reciprocal. The symbols (circles and squares in *Top* and *Bottom*, respectively) represent numerical results, and the solid lines (green and blue in *Top* and *Bottom*, respectively) show analytical results in the effective medium approximation. The red lines represent the light lines.

medium with reduced/increased effective ϵ or μ, rather than with respect to c_m.

Importantly, relativity imposes that the permittivity and permeability of a moving medium change at the same pace (21–23), as electric and magnetic effects are intimately linked to each other in relativity. Hence, the mapping to a moving medium can be done only in the case of space–time modulations of both ϵ and μ, whereas the moving medium interpretation fails if either material parameter is not modulated. This is a fundamental difference between systems where only one parameter (either the electric or the magnetic one) is modulated in space and time and systems which feature both modulations simultaneously and explains why the aether drag and nonreciprocity disappear for modulations of only ϵ or μ.

Nonreciprocal Dispersion Relations. We now discuss in detail the effective medium theory presented above and validate our analytical expressions against numerical results.

The nonreciprocal dispersion relations given by Eq. **20** are shown in Fig. 4 for a choice of nonzero electric and magnetic modulation amplitudes $\alpha_e = \alpha_m = 0.2$ (Fig. 4 *A* and *B*, *Top*, solid green lines). Numerical results obtained from Eq. **7** are also plotted with symbols, validating our effective medium theory. For waves propagating in the direction of the modulation ($k_y = 0$), the dispersion relations are linear, $k_\pm = (\delta \pm \beta)\omega$, as can be seen in the plot. In fact, when $\alpha_e = \alpha_m$, the eigenvalue Eq. **8** becomes block diagonal because $M^{EH} = M^{HE}$, such that $M^{+-} = M^{-+} = 0$, reflecting the fact that forward and backward waves do not interact in this case. Indeed this periodic system, being impedance-matched to free space at all positions x and times t, has zero band gaps at higher frequencies and momenta, as discussed in ref. 25. However, despite the fact that forward and backward waves do not interact with each other, the modulation acts on each of them, yielding a nonreciprocal response. The speed of forward and backward waves is in fact different, and, according to Eq. **20**, it is given respectively by

$$v_+ = \frac{\omega}{k_+} = c_m \left(1 + 2\alpha^2 \frac{c_g}{c_m - c_g}\right)^{-1}, \quad \text{[27]}$$

$$v_- = \frac{\omega}{k_-} = -c_m \left(1 - 2\alpha^2 \frac{c_g}{c_m + c_g}\right)^{-1}. \quad \text{[28]}$$

It is also clear from Eqs. **27** and **28** that for subluminal grating speeds ($c_g < c_m$), forward waves propagating through the space–time-modulated medium speed up and backward waves slow down, in agreement with a negative Fresnel drag velocity. In particular, $v_+ < c_m$ and $|v_-| > c_m$, such that the branch at $k > 0$ lies below the light line for the unmodulated material, and the branch at $k < 0$ lies above it, as can be seen in Fig. 4 *A*, *Top*. For the case of superluminal grating speeds ($c_g > c_m$), the speed of forward waves increases and that of backward waves decreases, in agreement with a positive Fresnel drag velocity. We remark here that while both velocities increase with respect to waves propagating in the absence of modulation ($v_+ > c_m$, $|v_-| > c_m$, both branches lie above the light line), the Fresnel drag in fact acts with respect to a medium with reduced effective permittivity and permeability (as given by Eq. **26**). In the superluminal case the phase velocity of waves in such medium is in fact reduced by a large amount, $\sim\Omega^2$, and the reciprocity breaking term is not strong enough to move the backward propagating branch to the opposite side of the light line. Hence, while the drag acts in the same direction for both sets of waves, both branches lie above the light line of unmodulated media (Fig. 4 *B*, *Top*). These different phase velocities for forward and backward modes are consistent with the results presented in Fig. 3, where $\Delta/2 = (v_g^+)^{-1} - (v_g^-)^{-1} = \delta$ is plotted.

On the other hand, if either the permittivity or the permeability is kept constant ($\alpha_{e/m} = 0.2$, $\alpha_{m/e} = 0$), the reciprocity-breaking term $\delta = 0$, and the dispersion relations are fully reciprocal in the long-wavelength limit, as shown in Fig. 4 *A* and *B*, *Bottom*. In this case, and for subluminal modulations, the forward/backward wave decreases/increases in speed with respect to c_m, and the dispersion relations lie below the light lines, and conversely for superluminal modulations, for which both branches lie above the light lines. The phase velocities are given by β^{-1} in this case, whose deviation from the unmodulated system is quantified by terms $\sim \Omega^2/(c_m^2 g^2 - \Omega^2)$. This explains why the effect is more pronounced for superluminal (Fig. 4 *B*) than for subluminal (Fig. 4 *A*) modulations and why for the superluminal case both branches remain above the light line with electric and magnetic modulations.

Finally, for off-normal incidence, $k_y \neq 0$, the dispersion presents a cutoff and exhibits the Fresnel drag by tilting toward the positive k direction for subluminal modulations and toward the negative one for superluminal modulations, in agreement with Fig. 2.

Transmission Line Model. We propose a realization of Fresnel drag in a transmission line comprising the discrete elements shown in Fig 5*A*, which can be modeled as detailed in *Materials and Methods*. We note that transmission lines have been used to test other phenomena appearing in moving media. In particular, nonlinear inductors were used to demonstrate the inverse Doppler effect by which waves reflect from a receding boundary with an increased frequency (29). In our setup, varactors are used, so that a strong pump signal can modulate their capacitance in time, with appropriate phasing from one varactor to another. Varactors are available with a typical capacitance of 100 pF. Both the inductive and the capacitive elements must be modulated to see the drag effect: Ferrite-core inductors, with inductance of the order of 1μH, are commercially available. The ferrite core has a nonlinear response, enabling the pump beam to vary the inductance. A powerful high-frequency pump signal is sent through the system to produce the required modulation of the elements, ensuring that the varactors are biased with a dc voltage greater than the modulation. Simultaneously, a low-frequency probe tests the effect of the modulation, as illustrated in Fig. 5*B*. For the values of inductance and capacitance
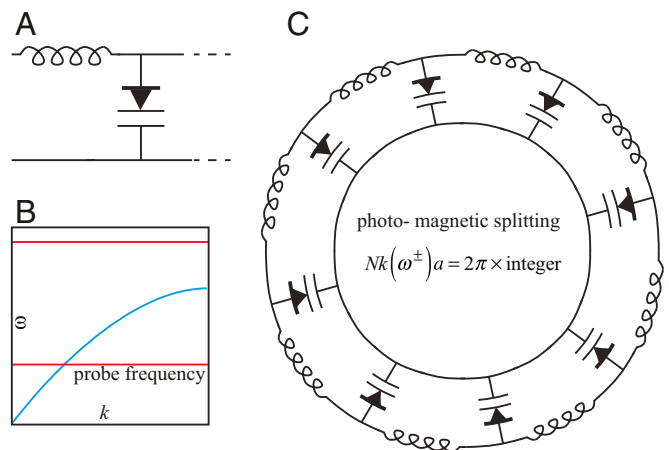

Fig. 5. (*A*) The capacitor in a conventional transmission line is replaced by a varactor, whose capacitance varies with the voltage across it. The inductors are also assumed to vary with the bias current. (*B*) Schematic dispersion showing the pump and probe frequencies. (*C*) Discrete elements combined into a loop to demonstrate the presence of a photomagnetic field.

quoted, the cutoff frequency of the transmission line would be approximately 6 MHz.

One suggestion for detecting the drag is to make an analogy with the electrons confined to a loop. In the absence of a magnetic field, nonzero angular momentum states are 2-fold degenerate, as dictated by time-reversal symmetry. A magnetic field breaks this symmetry and splits the formerly degenerate states. Fig. 5C shows the configuration. The loop quantizes the states, and the space–time modulation of the elements produces an effective gauge field for photons (30), resulting in a splitting of opposite-propagating modes, in analogy with the Zeeman splitting in atomic physics (24, 31).

In summary, we have shown that space–time-modulated systems can, in the low-frequency limit, be represented as bianisotropic metamaterials or alternatively as uniaxial metamaterials in motion relative to the observer's reference frame. In the latter case we claim that this is an instance of Fresnel's aether drag hypothesis but with the interesting twist that modulations of the system do not displace the physical medium itself and the motion is apparent rather than real. Further, the velocity of the modulations, c_g, is only indirectly related to the drag velocity, v_D, whose sign and magnitude can be changed by the size and relative phase of the electric and magnetic modulation amplitudes. Our system presents a rich variety of phenomena with parameters that are highly tunable.

We mention in passing that we expect realizations in other wave phenomena, such as acoustics, where both density and bulk modulus need to be modulated to achieve a Willis stress–velocity coupling parameter in the homogenization regime (32), to be possible. Finally, we suggest an electronic circuit model as a possible test bed for these ideas.

Materials and Methods

Matrices in the Bloch–Floquet Method. The matrices in the eigenvalue equation, Eq. 7, are given by

$$\mathbf{M}^{EE}_{n'n} = \mathbf{M}^{HH}_{n'n} = -ng\delta_{nn'},$$ [29]

$$\mathbf{M}^{HE}_{n'n} = -\epsilon_0 \left\{ \begin{array}{c} (\omega + n\Omega)\delta_{nn'} - k_y^2 c_m^2 \left(S^{EH}_{n'n}\right)^{-1} \\ +\alpha_e(\omega + n\Omega)(\delta_{n+1,n'} + \delta_{n-1,n'}) \\ +\alpha_e\Omega(\delta_{n+1,n'} - \delta_{n-1,n'}) \end{array} \right\},$$ [30]

$$\mathbf{M}^{EH}_{n'n} = -\mu_0 \left\{ \begin{array}{c} (\omega + n\Omega)\delta_{nn'} \\ +\alpha_m(\omega + n\Omega)(\delta_{n+1,n'} + \delta_{n-1,n'}) \\ +\alpha_m\Omega(\delta_{n+1,n'} - \delta_{n-1,n'}) \end{array} \right\},$$ [31]

with

$$\mathbf{S}^{EH}_{n'n} = \left\{ \begin{array}{c} (\omega + n\Omega)\delta_{nn'} \\ +\alpha_m(\omega + n\Omega)(\delta_{n+1,n'} + \delta_{n-1,n'}) \\ +\alpha_m\Omega(\delta_{n+1,n'} - \delta_{n-1,n'}) \end{array} \right\}.$$ [32]

Transmission Line. The elements in the transmission line in Fig. 5 vary in time as

$$C_n(t) = B_1 \left[1 + \alpha_1 \left(e^{+i(\Omega t + \theta_n)} + e^{-i(\Omega t + \theta_n)} \right) \right]^{-1},$$ [33]

$$L_n(t) = B_2 \left[1 + \alpha_2 \left(e^{+i(\Omega t + \theta_n)} + e^{-i(\Omega t + \theta_n)} \right) \right]^{-1}.$$ [34]

Solving the equations

$$\dot{V}_n = C_n^{-1}(I_n - I_{n+1}),$$ [35]

$$\dot{I}_{n+1} = L_{n+1}^{-1}(V_n - V_{n+1}),$$ [36]

it can be proved that our transmission line model reproduces the Fresnel drag when both elements are modulated.

1. A. Fresnel, Lettre d'Augustin Fresnel à François Arago sur l'influence du mouvement terrestre dans quelques phénomènes d'optique. *Ann. Chem. Phys.* **9**, 57–67 (1818).
2. H. Fizeau, Sur les hypothèses relatives à l'éther lumineux. *C. R. Acad. Sci.* **33**, 349–355 (1851).
3. A. Einstein, Zur elektrodynamik bewegter koerper. *Ann. Phys.* **322**, 891–921 (1905).
4. C. Caloz et al., Electromagnetic nonreciprocity. *Phys. Rev. Appl.* **10**, 047001 (2018).
5. C. Caloz, Z. Deck-Léger, Spacetime metamaterials, part I: General concepts. *IEEE Trans. Antennas Propag.*, 10.1109/TAP.2019.2944225 (2019).
6. J. N. Winn, S. Fan, J. D. Joannopoulos, E. P. Ippen, Interband transitions in photonic crystals. *Phys. Rev. B* **59**, 1551–1554 (1999).
7. H. Lira, Z. Yu, S. Fan, M. Lipson, Electrically driven nonreciprocity induced by interband photonic transition on a silicon chip. *Phys. Rev. Lett.* **109**, 033901 (2012).
8. S. A. Tadesse, M. Li, Sub-optical wavelength acoustic wave modulation of integrated photonic resonators at microwave frequencies. *Nat. Commun.* **5**, 5402 (2014).
9. E. Cassedy, A. Oliner, Dispersion relations in time-space periodic media: Part I—Stable interactions. *Proc. IEEE* **51**, 1342–1359 (1963).
10. E. Cassedy, Dispersion relations in time-space periodic media part II—Unstable interactions. *Proc. IEEE* **55**, 1154–1168 (1967).
11. F. Biancalana, A. Amann, A. V. Uskov, E. P. O'Reilly, Dynamics of light propagation in spatiotemporal dielectric structures. *Phys. Rev. E* **75**, 046607 (2007).
12. D. L. Sounas, A. Alù, Non-reciprocal photonics based on time modulation. *Nat. Photonics* **11**, 774–783 (2017).
13. T. A. Morgado, M. G. Silveirinha, Negative Landau damping in bilayer graphene. *Phys. Rev. Lett.* **119**, 133901 (2017).
14. T. T. Koutserimpas, A. Alù, R. Fleury, Parametric amplification and bidirectional invisibility in PT-symmetric time-Floquet systems. *Phys. Rev. A* **97**, 013839 (2018).
15. E. Galiffi, P. A. Huidobro, J. B. Pendry, Broadband nonreciprocal amplification in luminal metamaterials. *Phys. Rev. Lett.* **123**, 206101 (2019).
16. Y. Mazor, A. Alu, One-way hyperbolic metasurfaces based on synthetic motion. arXiv:1902.02653 (6 February 2019).
17. T. T. Koutserimpas, R. Fleury, Nonreciprocal gain in non-Hermitian time-Floquet systems. *Phys. Rev. Lett.* **120**, 087401 (2018).
18. A. Regensburger et al., Parity–time synthetic photonic lattices. *Nature* **488**, 167–171 (2012).
19. Q. Lin, M. Xiao, L. Yuan, S. Fan, Photonic Weyl point in a two-dimensional resonator lattice with a synthetic frequency dimension. *Nat. Commun.* **7**, 13731 (2016).
20. R. Fleury, A. B. Khanikaev, A. Alu, Floquet topological insulators for sound. *Nat. Commun.* **7**, 11744 (2016).
21. L. He et al., Floquet Chern insulators of light. *Nat. Commun.* **10**, 4194 (2019).
22. Z. Yu, S. Fan, Complete optical isolation created by indirect interband photonic transitions. *Nat. Photonics* **3**, 91 (2009).
23. D. L. Sounas, C. Caloz, A. Alu, Giant non-reciprocity at the subwavelength scale using angular momentum-biased metamaterials. *Nat. Commun.* **4**, 2407 (2013).
24. N. A. Estep, D. L. Sounas, J. Soric, A. Alù, Magnetic-free non-reciprocity and isolation based on parametrically modulated coupled-resonator loops. *Nat. Phys.* **10**, 923–927 (2014).
25. S. Taravati, Giant linear nonreciprocity, zero reflection, and zero band gap in equilibrated space-time-varying media. *Phys. Rev. Appl.* **9**, 064012 (2018).
26. J. A. Kong, *Electromagnetic Wave Theory* (Wiley- Interscience, New York, NY, 1986).
27. J. Vehmas, S. Hrabar, S. Tretyakov, Transmission lines emulating moving media. *New J. Phys.* **16**, 093065 (2014).
28. M. G. Silveirinha, Spontaneous parity-time-symmetry breaking in moving media. *Phys. Rev. A* **90**, 013842 (2014).
29. N. Seddon, T. Bearpark, Observation of the inverse Doppler effect. *Science* **302**, 1537–1540 (2003).
30. K. Fang, Z. Yu, S. Fan, Realizing effective magnetic field for photons by controlling the phase of dynamic modulation. *Nat. Photonics* **6**, 782–787 (2012).
31. R. Fleury, D. L. Sounas, C. F. Sieck, M. R. Haberman, A. Alù, Sound isolation and giant linear nonreciprocity in a compact acoustic circulator. *Science* **343**, 516–519 (2014).
32. H. Nassar, X. Xu, A. Norris, G. Huang, Modulated phononic crystals: Non-reciprocal wave propagation and Willis materials. *J. Mech. Phys. Solids* **101**, 10–29 (2017).